Cut-off Characterization of Bright Fermi Sources: Current instrument limits and future possibilities.

C. Romoli, A. M. Taylor, F. Aharonian

Abstract

In this paper we analyse some of the brightest GeV sources seen by the *Fermi*-LAT, focusing on the cutoff region of their spectra. An attempt is made to reconstruct the underlying particle distribution giving rise to this emission. Reasonable constraints on the parameters describing their cutoffs were found for only the two brightest objects from our sample sources, namely the Vela pulsar and the 2010 flare of the blazar 3C 454.3. Despite these present limitations, we highlight the benefits of such a study soon to be brought about by next generation of ground based Cherenkov telescopes, represented by the Cherenkov Telescope Array. Adopting current effective area and PSF simulations, we describe the great potentialities in terms of count rate and time resolution for this new instrument when compared with satellite performances.

1. INTRODUCTION

A range of both galactic and extragalactic objects are known to be effective particle accelerators. The end of the non-thermal tail, in the particle spectra produced, contains important informations about the nature of the accelerator. This part of the spectrum can be described with a power law with a stretched/compressed exponential cutoff (PLSEC). This function is characterized by having an additional parameter β which determines the steepness of the cutoff (stretched for $\beta < 1$, compressed for $\beta > 1$):

$$\frac{dN}{dE} = N_0 \left(\frac{E}{E_s}\right)^{-\alpha} \exp\left(-\left(\frac{E}{E_c}\right)^{\beta}\right) \tag{1.1}$$

where E_s indicates the energy scale of the power law region[1] and E_c the cut-off energy.

According to the analytical models of particle acceleration, a β_e parameter for the electrons, naturally arises when considering energy losses. As an example Zirakashvili & Aharonian (2007) have shown that, in case of particle acceleration challenged by radiative losses proportional to E^2, like synchrotron or inverse Compton in Thomson regime, the outcome is a compressed exponential cut-off with $\beta_e = 2$. Other possible values can be obtained in the framework of stochastic acceleration with the cut-off shape related to the turbulence spectrum. A rather complete analysis has been

[1] In the fitting of the *Fermi*-LAT data this parameter has been fixed to the value reported in the 2FGL catalogue (Nolan et al. 2012).

done by Stawarz & Petrosian (2008). They showed that when the escape losses can be neglected, the particle spectrum that arises from the balance between the acceleration and the radiative losses is characterized by a stretched cut-off with the parameter β_e that can be written, in a general form, as $\beta_e = 2 - q - r$ where r is the index of the dependence of the time-scale of the losses with the particle energy ($t_{loss} \propto E_e^r$) and q is the spectral index of the turbulence power spectrum defined as $W(k) \propto k^{-q}$, where k is modulus of the wave-number vector[2].

The effect of β is to modify the cutoff, and consequently the resultant photon spectrum emitted. For the case of synchrotron emission the output is a spectrum with a cut-off dictated by a β parameter given by $\beta = \frac{\beta_e}{\beta_e+2}$ (Fritz 1989), indicating that a cutoff with a compressed exponential shape is incompatible with a synchrotron origin.

When we deal instead with inverse Compton processes, the emitted spectrum of the scattered photons is affected by the electron distribution and the target photon field. The outcome is also affected by the cross section of the interaction with a different behaviour going from the Thomson ($\varepsilon_e \varepsilon_\gamma^{bg} \ll \left(m_e c^2\right)^2$) to the Klein-Nishina ($\varepsilon_e \varepsilon_\gamma^{bg} \gtrsim \left(m_e c^2\right)^2$) regime. The analysis of the various processes has been done by Lefa et al. (2012) taking into account different photon fields. They showed that in the Klein-Nishina regime, due to the fact that the electron loses almost all of its energy in the interaction with the photon, the spectrum of the latter particle resembles the spectrum of the electrons, showing the same β parameter. In the Thomson regime, instead, the photon spectrum is always stretched with $\beta < \beta_e$.

Objects for which this cutoff sits in the GeV domain, presently may be most effectively probed by the Large Area Telescope (LAT) onboard the *Fermi* satellite. This is a pair conversion telescope capable of reconstructing the direction and the energy for incoming photons between 20 MeV and more than 300 GeV (Atwood et al. 2009).

In this work we analysed a small sample of some of the brightest objects observed by the *Fermi*-LAT. We studied the emission from a steady source such as the Vela pulsar and bright flares coming from different typology of gamma ray emitters such as AGN, PWNe and binary systems. Utilizing Fermi data, the spectra of bright objects with the highest statistic in the GeV range are used to constrain the photon spectral shape in the cut-off region as a tool for probing the acceleration, escape, and radiative loss processes giving rise to the particle energy distribution in this region. The list of these object is in table 1 with the indication of the time window analysed.

---

[2] $q = 1$ for the Bohm diffusion, $q = \frac{3}{2}$ for a Kraichnan spectrum, $q = \frac{5}{3}$ in the Kolmogorov case and $q = 2$ for the "hard-sphere" approximation

Table 1:: Sources and type of event analysed.

Object	Class	Event type	Analysed Period
3C 454.3	AGN (FSRQ)	Flare	Nov. 2010
3C 279	AGN (FSRQ)	Flare	Nov. 2008 - March 2009
Crab Nebula	PWN	Flare	April 2011
Vela X	Pulsar	Averaged emission	Aug. 2008 - Oct. 2013
PSR B1259-63	Binary pulsar	Flare	Jan. 2011

2. ANALYSIS OF THE *Fermi*-LAT DATA

The analysis of the *Fermi*-LAT data was performed using the Science Tools v9r27r1[3] and the Instrument Response Functions (IRFs) "P7SOURCE_V6" provided by the *Fermi* collaboration[4].

The gamma ray emission from all the sources was investigated between 100 MeV and 300 GeV energies using the `gtlike` routine to maximize the binned likelihood function (Mattox et al. 1996). The data were extracted from a square region $30^\circ \times 30^\circ$ centred in the position given by the 2FGL catalogue (Nolan et al. 2012). Only for the Vela pulsar was a smaller (20°) square region adopted.

The source parameters were obtained fitting a model for each Region of Interest (RoI). These models contain the contribution of all the sources within a radius large of a semi-side of the RoI plus 5 degrees. This extra contribution is due to the large PSF of the instrument at low energy. While the emission of all the sources inside the RoI has been fitted with the likelihood procedure, the sources outside the RoI had the parameters fixed to their 2FGL value. To take into account the diffuse emission we used the *Fermi* templates `iso_p7v6source` and `gal_2yearp7v6_trim_v0` for the isotropic and galactic diffuse emission[5] respectively. For the analysis of the Vela pulsar, due to a much longer integration time compared with the 2FGL catalogue, we added to the model two new sources called BkgA and BkgB, as suggested by (Hewitt et al. 2012) and (Grondin et al. 2013).

After a first fit to fix the background sources, the spectral points were obtained by fitting the central source with a simple power law and storing the normalization value in each energy bin. The SED points were computed for sources with a significance level (TS) of at least 9 ($\sim 3\sigma$) in each bin. Otherwise a 95% upperlimit was plotted. The error bars computed with the Science Tools are the Gaussian approximation of the Poissonian statistic (using the square root of the number of counts). This approach is incorrect in case of a very small number of photons in the bin. For this reason, if the number of photons in the energy bin is less than 10, we used as error bars the $1\,\sigma$

[3] `http://fermi.gsfc.nasa.gov/ssc/data/analysis/software/`

[4] `http://www.slac.stanford.edu/exp/glast/groups/canda/archive/pass7v6/lat_Performance.htm`

[5] `http://fermi.gsfc.nasa.gov/ssc/data/access/lat/BackgroundModels.html`

confidence interval proper of the Poissonian theory that can be found in Gehrels (1986).

Since very bright sources are adopted for our study, the statistical errors are generally much smaller than the systematic uncertainty associated to the detector. These errors, therefore, need also be taken into account. We used in our analysis the systematic uncertainties due to the effective area. According to the *Fermi* collaboration, for the used set of IRFs, these are at the 10% level at 100 MeV, 5% at 560 MeV and 10% from 10 GeV to 100 GeV[6]. In order to be conservative we transferred this information on the SED points (Ackermann et al. 2012) adding it in quadrature to the statistical uncertainty to obtain an estimate of the total error.

The SEDs were then fitted with a power law with a stretched/compressed exponential cut-off in the same form as (1.1).

Systematic uncertainties dominate at low energies, whilst at higher energies statistical uncertainties dominate, as visible in the plots 1 and 3. This affects the possibility to obtain good constraints on the fit parameters. The result is that for only two objects we were able to constrain the value of the β parameter: the flaring phase of 3C 454.3 and the Vela pulsar, shown in the following subsections.

2.1. Vela pulsar

The Vela pulsar is the brightest pulsar in the GeV energy range. In our analysis we used the averaged emission of the pulsar over more than 5 years of data, starting from the beginning of the *Fermi* data taken (MJD 54682.655) to MJD 56589.096.

Due to the large amount of data collected by the *Fermi*-LATfor this object, the corresponding spectral parameter constraints obtained were the strongest of those found for all the sources considered. The PLSEC fit gives $N_0 = (5.2 \pm 3.6) \times 10^{-5}$ ph/(cm^2 s GeV), $\alpha = 0.9 \pm 0.2$, $E_c = 0.1 \pm 0.1$ GeV and $\beta = 0.42 \pm 0.06$ with an overall $\chi^2_{red} = 0.46$. In figure 1 we show the computed SED with the best fit PLSEC and the 1σ contour. Even taking into account the systematic errors, we can exclude the possibility of a simple exponential function. We can therefore rule out the hypothesis of a photon spectrum generated by monoenergetic electrons with an isotropic distribution of pitch angle, giving rise to $\beta = 1$.

Another aspect that arises from the fitted function is the role of the cut-off energy E_c, which for the case of $\beta < 1$ moves to lower energies and does not correspond anymore to the peak of the SED plot. For the Vela pulsar, the peak energy is around 1 GeV, but the reconstructed cut-off energy is even below the first data point in the computed SED, although the value is not well constrained, with $E_c = 0.1 \pm 0.1$ GeV being obtained. This inability to constrain the cut-off energy parameter follows as a result of the cut-off energy sitting outside (below) the data point energy range.

---

[6] `http://fermi.gsfc.nasa.gov/ssc/data/analysis/LAT_caveats_pass7.html`

If we consider this spectrum as the result of synchrotron emission, we can also derive the β_e parameter of the electron distribution given that $\beta = \frac{\beta_e}{\beta_e+2}$. The reconstructed value is 1.5 ± 0.4.

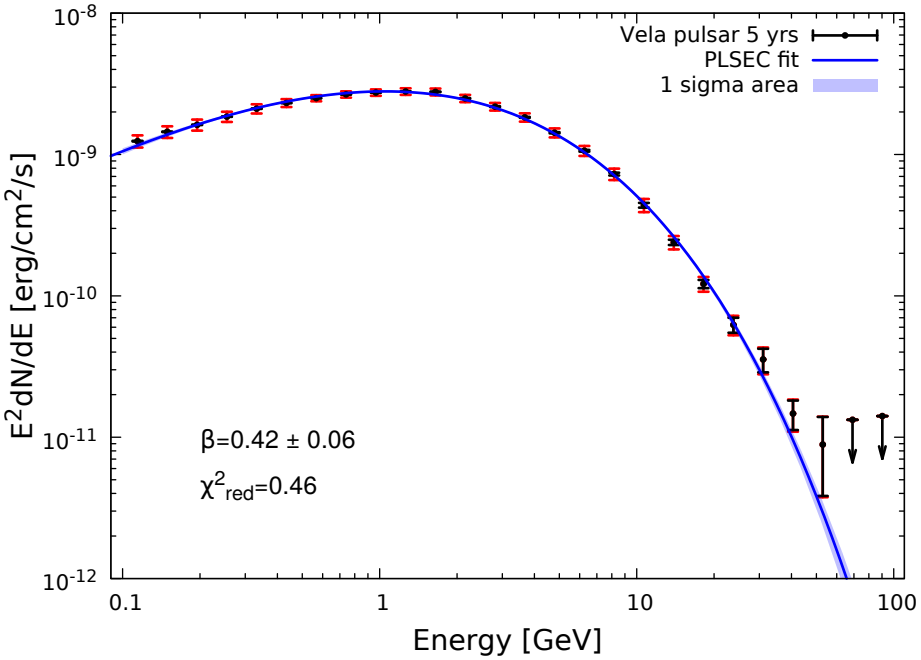

Fig. 1.—: SED for the Vela pulsar fitted with a power law with sub-exponential cut-off, The shaded area that is the 1σ contour. We indicated also the value of the reduced χ^2 and the value of the β parameter. The statistical errors are indicated with the black error bars while the red bars are the sum of the statistical and systematic errors on the SED point.

Following this phenomenological analysis based only on the fit of the simple photon spectra, we have tried to derive it starting directly from the distribution of the accelerated particles assuming again a power law with a stretched/compressed exponential cut-off. The method used to obtain the results was a Markov Chain Monte Carlo (MCMC) with a random walker based on the Metropolis-Hastings algorithm (Hastings 1970). The effectiveness of this technique in exploring the parameter space is in the possibility to accept the value of a set of parameters even if this brings about an increase of the χ^2, allowing the sampler to escape from local minima. The set of values of the parameters that minimise the χ^2 is chosen as the *best fit*. Looking at the distribution of the χ^2 during the various Monte Carlo trials as a function of one of the parameters, it is possible to also find the associated uncertainty of a given parameter.

For the Vela pulsar we started with a simple synchrotron model assuming a uniform magnetic field of strength $B = 1$ G. The result of the obtained MCMC fit is shown in figure 2. The results we are mostly interested in are the position of the cut-off and its steepness. From the plot one may directly appreciate how well this simple synchrotron model can fit the data. The value obtained

for the cut-off in the electron spectrum is $E_c = 150 \pm 0.15$ TeV with an exponent for the steepness $\beta_e = 2.05 \pm 0.25$. Unfortunately, the cut-off energy is degenerate with the value of the magnetic field adopted. However, one can write that the Vela pulsar is able, in a simple synchrotron scenario, to accelerate electrons up to energies of $(150 \pm 0.15) \left(\frac{B}{1\ \mathrm{G}}\right)^{-1/2}$ TeV, for which the dependence on the cut-off energy and magnetic field strength parameters is stated explicitly.

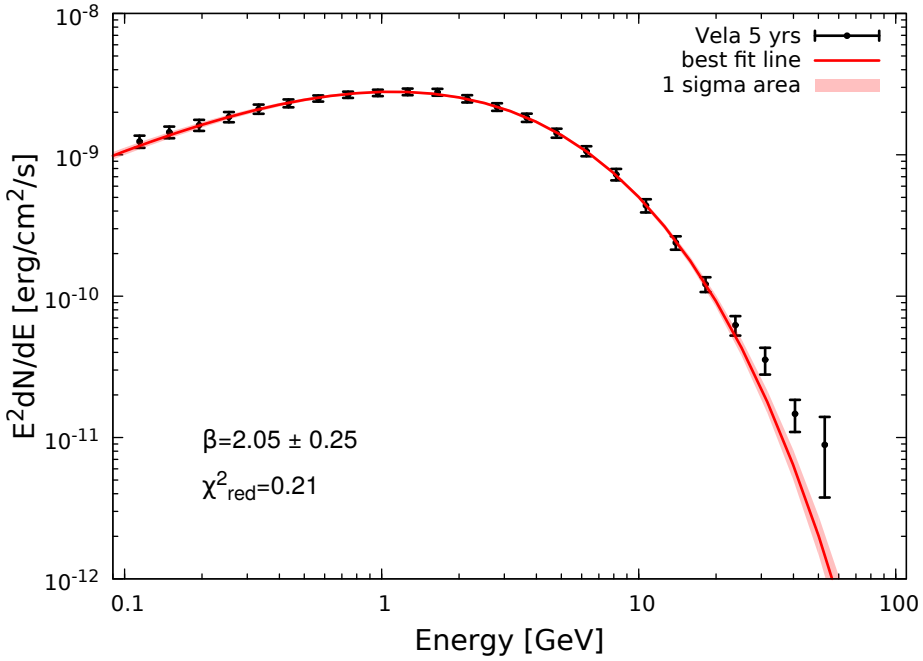

Fig. 2.—: *Fermi*-LAT spectrum of the Vela pulsar with superimposed the best fit line from the synchrotron model. The area in red is the 1σ area around the best fit value. In the graph is reported also the value of the β parameter for the electrons and the reduced χ^2 of the fit.

2.2. 3C 454.3

We applied the same procedure of that outlined in the previous section to the flare of the blazar 3C 454.3. This is the brightest AGN in the GeV band observed by *Fermi*-LAT. Specifically, we analysed the very bright flare detected in the November 2010 when the source reached an integrated flux level of $\sim 8 \times 10^{-5}$ ph cm^{-2} s^{-1}. To study the spectral evolution during the flare, we used the same time intervals defined by Abdo et al. (2011). The produced SEDs are in figure 3 where we also show the fit of the PLSEC with the 1σ contour. The analysis cannot constrain the β parameter for all the periods. Only for the flaring phase we end with a value of $\beta = 0.4 \pm 0.3$. In the pre-flare, plateau and post-flare phase the minimizer does not reach a convergence with this extra degree of freedom and for this reason, in those intervals, we fixed it to the value of 0.3, a good compromise to match the flatness of the spectrum.

Using the argument of Zirakashvili & Aharonian (2007), the value of β we found would be perfectly compatible with a cut-off in the electron spectrum steepened with a $\beta_e = 2$ as a result of the balance between acceleration and energy losses proportional to E^2. Due to the high Compton dominance observed in the source emission, as it appears in (Wehrle et al. 2012), we could link these losses to IC processes dominated by the Thomson regime. Unfortunately the constraint is not very strong and the possibility to have a simple exponential cut-off cannot be strongly rejected. To test

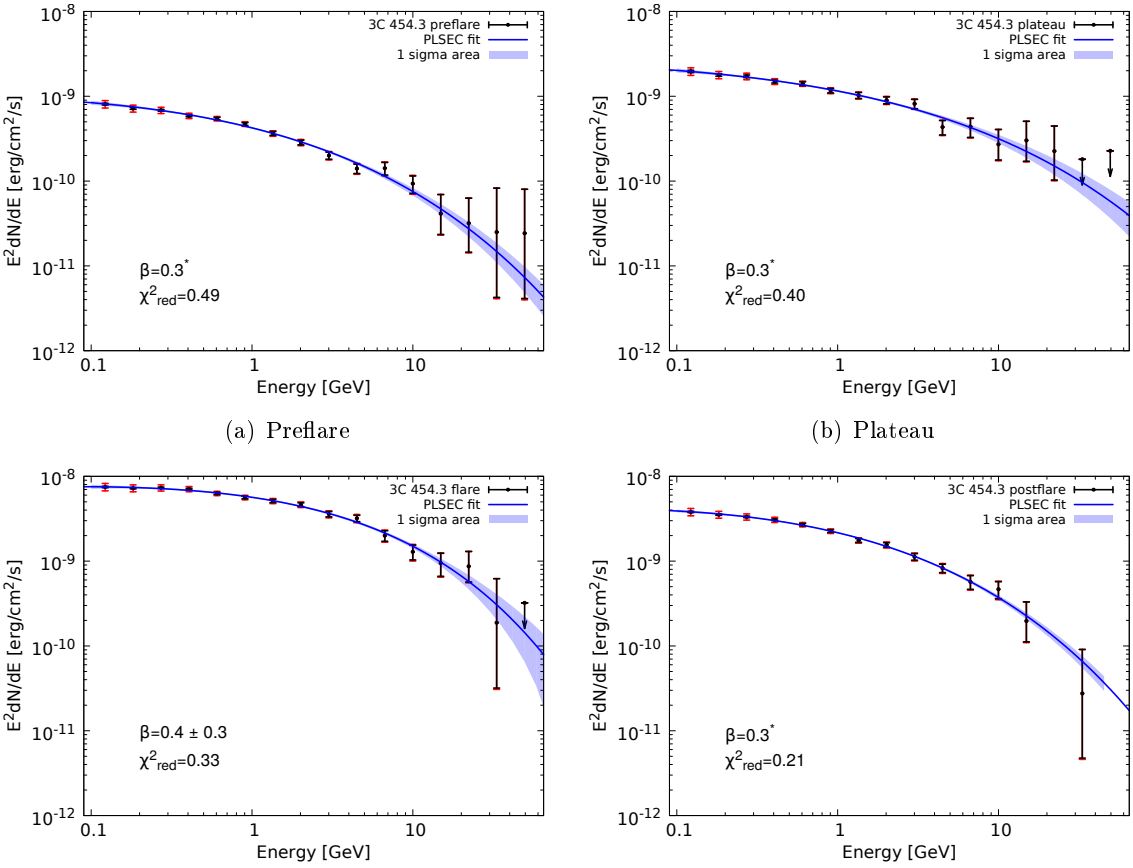

(a) Preflare (b) Plateau

(c) Flare (d) Post Flare

Fig. 3.—: SED for 3C 454.3 fitted with a power law with sub-exponential cut-off and the shaded area that is the 1σ contour. We indicated the value of the reduced χ^2 and the value of the β parameter, labelled with a star when it was not possible to constrain it. The statistical errors are indicated with the black error bars while the red bars are the sum of the statistical and systematic errors on the SED point.

the possibility to constrain the electron spectrum also for this source, we performed the MCMC routine assuming a simple SSC model and a uniform magnetic field $B = 1\,\mu$G, for a distribution of electrons with a compressed exponential cut-off. As already shown, in this case the statistical errors are sufficiently large to prevent a good determination of the values. From the fit results we

obtain a position for the cut-off, with the chosen magnetic field of 1 μG, of $E_c = 380^{+10}_{-90}$ GeV and the parameter $\beta_e = 2.65^{+0.5}_{-1.0}$. We neglected the effects of the cosmological redshift and of the jet boosting because we are mostly interested in the constrain possibility than in the absolute value of them (**RE-ELABORATE THIS it is to remember that these effect are not included yet**). These value are in agreement with the values found from the fit of the photon spectrum alone, having the Inverse Compton process in the Thomson regime even if the global uncertainty on β_e is quite large.

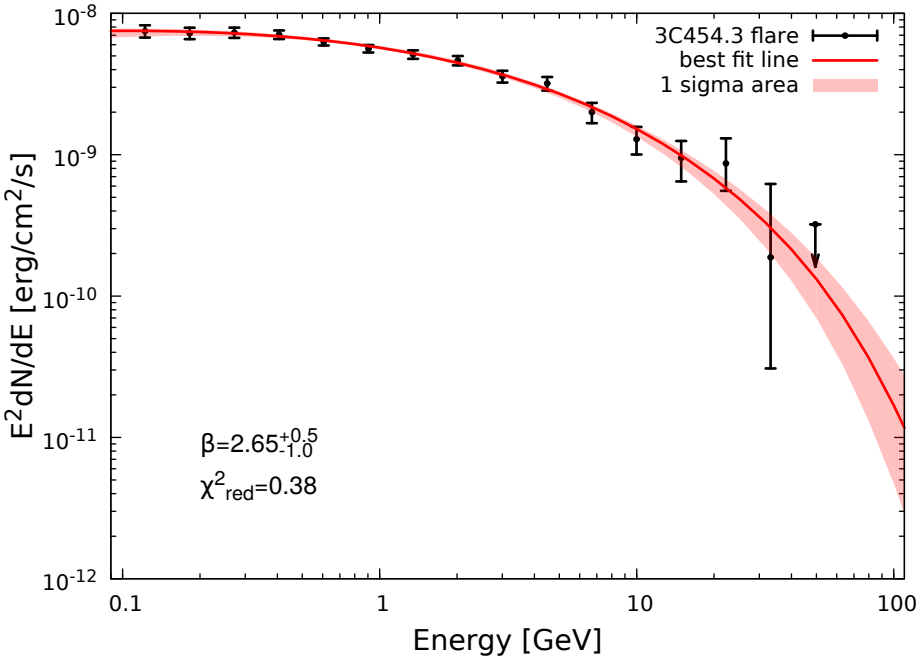

Fig. 4.—: *Fermi*-LAT spectrum of the flaring phase of the blazar 3C 454.3 with superimposed the best fit line from the SSC model. The area in red is the 1σ area around the best fit value. In the graph is reported also the value of the β parameter for the electrons and the reduced χ^2 of the fit.

3. FUTURE POTENTIAL OF IACTs AT 10 GeV

The possibility to more sensitively explore the cut-off region of GeV sources may be brought about through an increase effective area of the γ-ray instrument. This can be achieved through a lowering of the energy threshold of ground based Cherenkov telescope. These instruments have already proven themselves to be able to reach a minimum energy close to few tens of GeV under

particular conditions as shown by MAGIC (Doro & MAGIC Collaboration 2012) and HESS[7]. In this section we demonstrate the improvement possible through such an increasing in the effective area at energies around 10 GeV, for our bright *Fermi* sources.

The idea of pushing the energy threshold of the IACTs to energies below ~ 10 GeV has already been explored in the potential future Cherenkov telescope array, 5@5 (Aharonian et al. 2001). In their design, the array consisted of 5 big (~ 20 m of diameter) Cherenkov telescopes at an altitude of 5 km above the sea level, providing the opportunity to reach down to an energy of 5 GeV.

In the near future, construction of the *Cherenkov Telescope Array* (CTA) is planned. This will consist of two observatories, one in the northern hemisphere, more dedicated to the study of extragalactic objects, and one in the southern hemisphere, more focused on the galactic plane. Each of them will be made of several Cherenkov telescopes of various diameters to explore different energy bands of the gamma ray spectrum as described by Actis et al. (2011).

In our study we will focus on the application of our results to CTA, according to preliminary design studies.

The construction site, at the moment of writing, has not yet been decided upon, with several investigations still ongoing to determine a suitable location taking into account altitude, strength of the geomagnetic field, atmospheric conditions. One of the candidates is in the Argentinian province of Salta. Due to the 3.6 km altitude above the sea level and the low strength of the geomagnetic field, a detailed study by Szanecki et al. (2013) highlights this site as one of the best to study lower energies with the IACT techniques. Hereafter we will use the computed collection area to explore the potential data quality we could obtain for the *Fermi*-LAT bright sources if they were observed with a low energy IACT.

In figure 5 we show the collection area computed by Szanecki et al. (2013) for the Salta site, comparing it with the one computed for the 5@5 project. One can already appreciate the potentiality of the instrument with respect to the *Fermi* satellite. The case in favour of ground based telescopes is in the much larger effective area: while *Fermi* can count only ~ 1 m^2 at 10 GeV, due to the Cherenkov light pool having a radius of ~ 100 m, a ground based telescope can in principle detect 10000 more photons in the same time interval.

Using the effective area, in combination with the source flux, we can compute the expected count rate at the detector. However one still has to take into account the background contamination present for this kind of instrument. At energies around 10 GeV one of the main background contaminants is the cosmic ray electron flux. Due to the fact that they generate, in the interaction with the atmosphere, an electromagnetic cascade very similar to those generated by gamma rays, this flux cannot be easily rejected either at trigger level or in an analysis filter, as is done for hadronic

[7]preliminary result on the detection of the Vela pulsar at 30 GeV. Reported in the news of 27 June 2014 in `https://www.mpi-hd.mpg.de/hfm/HESS/`

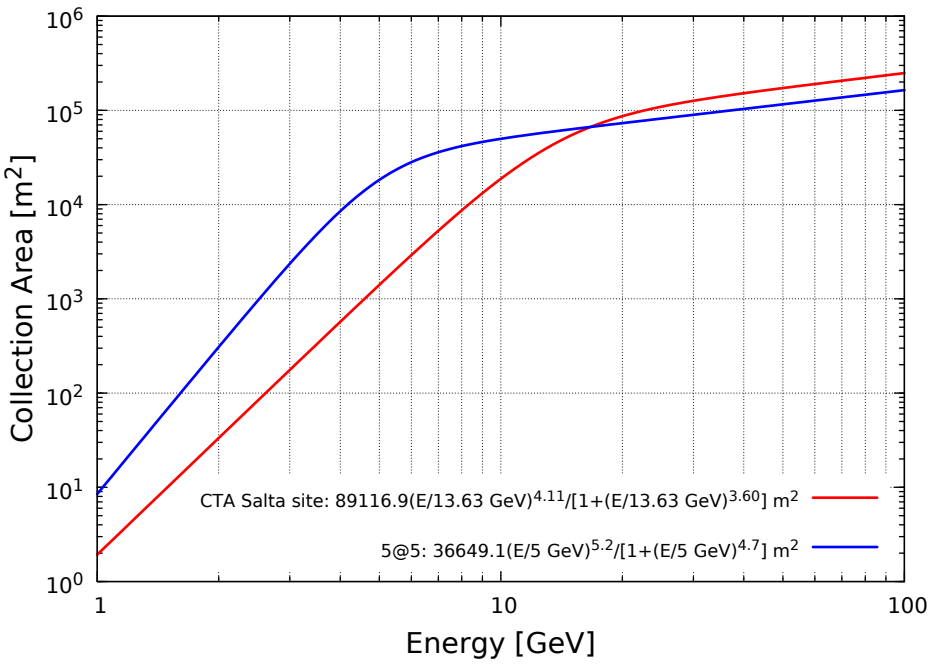

Fig. 5.—: Collection area for the CTA Salta site (Szanecki et al. 2013) and for the 5@5 IACT project (Aharonian et al. 2001). In the legend we report also the parametrization of both curves. See the respective articles for the details on the design chosen to derive these curves.

showers. To approximate the electrons flux in the energy range between few GeV and 100 GeV we used the parametrization adopted by Supanitsky & Rovero (2012) fitting the PAMELA and Fermi data:

$$\frac{dJ_e}{dEd\Omega} = \begin{cases} 1.12439 - \frac{22.2423}{E} + \frac{142.483}{E^2} - \frac{90.850}{E^3} & E \leq 7 \text{ GeV} \\ 256.183E^{-3.1213} & E > 7 \text{ GeV} \end{cases} \quad \text{m}^{-2}\ \text{s}^{-1}\ \text{GeV}^{-1}\ \text{sr}^{-1} \tag{3.1}$$

The background contamination has to be studied inside the PSF of the instrument and to approximate it we use the one simulated by Szanecki et al. (2013), parametrized as:

$$\phi = 0.58 \left(\frac{E}{1 \text{ GeV}} \right)^{-0.37} \text{ degree}. \tag{3.2}$$

First we test the background effect on a hypothetical source with a normalized energy flux of 10^{-9} erg/cm^2/s at 10 GeV, with power law spectra of photon indices -2,-3 and -4. This flux normalization value corresponds to that observed during the 3C 454.3 flare in 2010. The plot in figure 6 shows the comparison between the flux of the source and the flux of the diffuse electrons inside the PSF of the instrument. One can see how, for such high fluxes, we are "background free", with the source count rate always being above that of the electrons.

To have a better feeling of the transition between the background free and background dominated regimes, depending on the flux level of the source, we took the $\alpha = -2$ (red) curve in figure

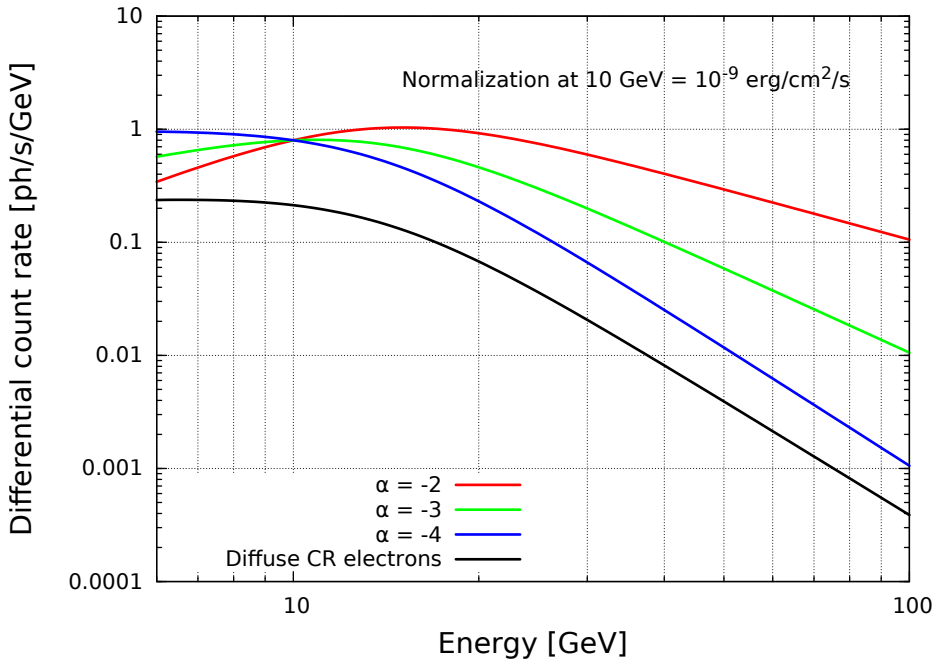

Fig. 6.—: Effect of the effective area in figure 5 in terms of expected differential count-rate, on a power-law spectrum with photon index $\alpha = -2$ (red), -3 (green), -4 (blue). In black there is the expected count rate for the diffuse CR electrons inside the PSF of the instrument.

6, scaling it by 0.1 and 0.01, focusing on the energy of the transition. In figure 7, we show that even for lower flux (0.01), hard spectra ($\alpha = 2$) cases, one may still in principle be able to detect the source.

With this general framework, we can apply these results to our set of sources, taking only those that have considerable signal above 10 GeV, excluding then the PSR B1259-63 flare and the Crab Nebula flare, both of which posses cutoffs too low in energy to consider ($\sim$ 1 GeV) (Buehler et al. 2012) (Tam et al. 2011). In figure 8 we show the detection rates for the example of the two flaring AGN and of the steady Vela pulsar. The shaded areas are the expected standard deviation on the differential count rates. As one can clearly see, for these bright objects, already after 10 hours of observations, the expected uncertainty on the flux would be much smaller than in the *Fermi*-LAT after an integration time of more than a week. In particular, with 3C 454.3 being in the signal dominated region, one would have an exceptional determination of its flux. This fact can open the possibility to study variability with a time resolution of few seconds and could open the gates for a revolution in our understanding of transient phenomena. We could even see a new record in the variability timescale beyond the $\sim$ 3 minutes registered by HESS in 2006 for the blazar PKS 2155-304 (Aharonian et al. 2007). A phenomenon that is already challenging to explain. Even for the flare of 3C 279, considering that we are in the background dominated regime, we would get a level of statistic far better than that obtained by Fermi. For sources like the Vela pulsar, the

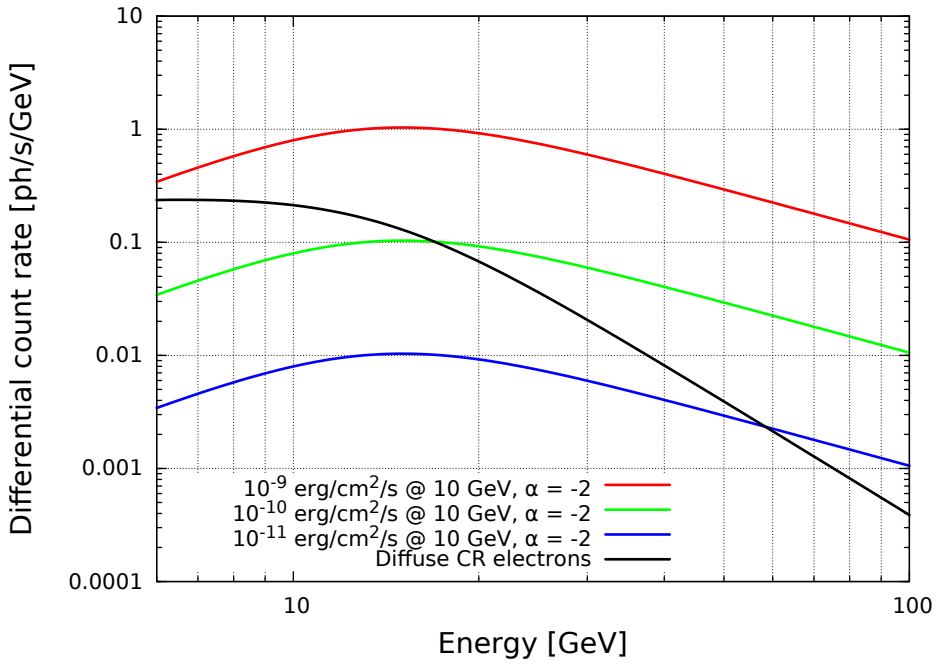

Fig. 7.—: Expected differential count rate a power law source with photon index $\alpha = -2$ and energy flux at 10 GeV of 10^{-9} (red), 10^{-10} (green), 10^{-11} (blue) erg/cm^2/s. In black is shown the expected differential count rate for the diffuse CR electrons inside the PSF of the instrument.

effect of the background would become relevant only at energies above 40 GeV, where the flux level becomes very low and comparable with that of the electrons.

This analysis does not take into account the full systematic uncertainty effects that might arise for the complete instrument, nor does it take into account the effect of observations at different zenith angles or in the presence of geomagnetic fields. All these factors would push the energy threshold toward higher energies (the magnetic field case has been studied in detail by (Szanecki et al. 2013)). Such considerations, however, are beyond the scope of this paper and if we look at figures 6,7 and 8 we can see how even with a 20 GeV threshold, one can still obtain precious new information about the end point of the spectrum of bright GeV sources.

4. CONCLUSIONS

In this paper we investigated the spectral shape and the position of the cut-off for a sample of some of the brightest sources seen by the *Fermi*-LAT. Even for this bright source subset, only a couple of objects were found to be sufficiently bright such that meaningful constraints on the parameter values could be obtained, namely only for the Vela pulsar and the the extreme flare of the blazar 3C 454.3. Following this analysis, an attempt to recover the underlying electron

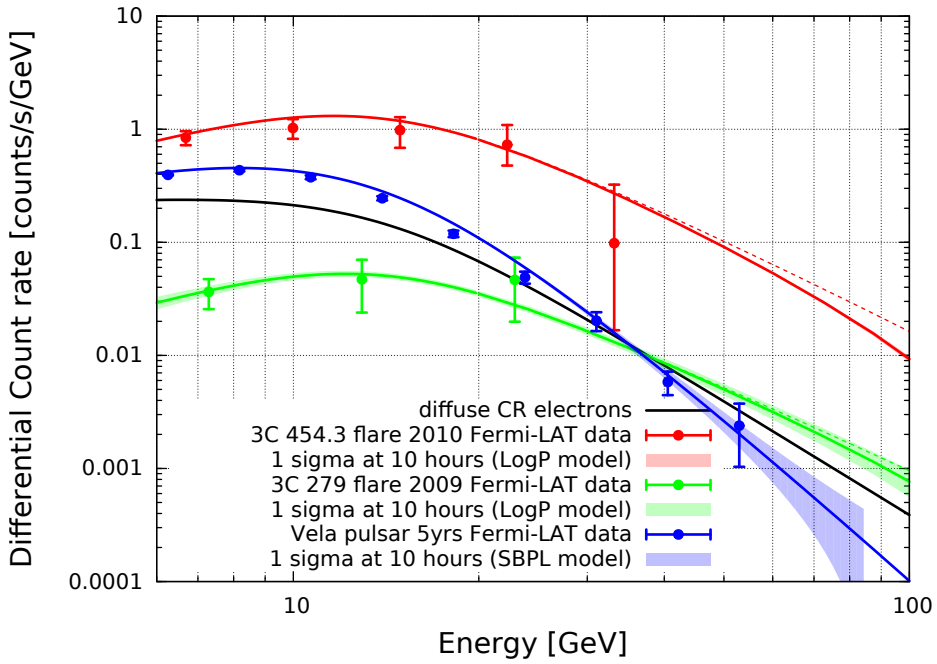

Fig. 8.—: Expected differential count rate for 3C 454.3, 3C 279 and the pulsar Vela. The data points are from the *Fermi*-LAT and the black line is the background level of the diffuse cosmic ray electrons. The solid lines are the best fit model to the data (log parabola for the two AGN and smooth broken power law for the Vela pulsar). Due to the high redshift, for the AGN the best fit line has been extrapolated up to 100 GeV taking into account the EBL absorption as estimated by Franceschini et al. (2008). The thin dashed line is the extrapolation of the unabsorbed spectrum. The shaded area around the best fit lines represents the expected standard deviation area on the count rate for the new instrument after 10 hours of observation.

energy distribution giving rise to this emission was made. For this study, a power law with a stretched/compressed exponential cut-off was adopted, to better describe the cut-off region of the electron distribution. For the Vela pulsar, due to the very high quality of the data, we were able to describe the photon spectrum as originating from synchrotron emitting electrons. The cut-off energy and steepness determination values obtained for this model, adopting a fixed magnetic field strength, were constrained with 10% uncertainty.

The case of 3C 454.3 was more involved. Furthermore, only 1 week of data was used in the analysis, corresponding to the peak of the 2010 flare. Due to the lack of statistics above 10 GeV, the constraints on the parameters, were much weaker. The SSC model we used to fit the data was unable to be strongly constrained, with weak limits on the steepness of the cut-off allowing a wide range of possible values for these parameters.

The aim of our study here was to demonstrate the significant potential that bright GeV objects

possess with regards studies of their underlying particle spectra, and the current limitation present instruments place on these studies. While for steady sources the continuous observation by the *Fermi*-LAT can give high quality data, for flaring objects the case is different. The limiting factor here being a lack of sufficient statistics in case of transient sources for energies above 10 GeV. Indeed, although the *Fermi*-LAT has contributed in a decisive way in our knowledge of the High Energy range, it is intrinsically limited by its small effective area that is around 1 m^2.

We then explored the benefits promised by an IACT system with a threshold in this energy range. As a reference, we used simulations for the near future of the field: the Cherenkov Telescope Array (CTA) that will be operative within the next few years. We applied simulations for its effective area and angular resolution to the real data coming from our set of bright GeV sources. In particular, for the bright objects we analysed, the statistical uncertainty after a 10 hours observation will already be small enough in order to put strong constraints on the spectral shape, with a level of statistic comparable to that of *Fermi*-LAT after years of data taking. Furthermore with the high expected count rate for extreme objects like 3C 454.3, CTA may open the gates for a revolution in our understanding of transient objects at high energies.

REFERENCES

Abdo, A. A., Ackermann, M., Ajello, M., et al. 2011, ApJ, 733, L26

Ackermann, M., Ajello, M., Albert, A., & Allafort, A. e. a. 2012, ApJS, 203, 4

Actis, M., Agnetta, G., Aharonian, F., et al. 2011, Experimental Astronomy, 32, 193

Aharonian, F., Konopelko, A., Völk, H., & Quintana, H. 2001, Astroparticle Physics, 15, 335

Aharonian, F., Akhperjanian, A. G., Bazer-Bachi, A. R., et al. 2007, ApJ, 664, L71

Atwood, W. B., Abdo, A. A., Ackermann, M., et al. 2009, ApJ, 697, 1071

Buehler, R., Scargle, J. D., Blandford, R. D., et al. 2012, ApJ, 749, 26

Doro, M., & MAGIC Collaboration. 2012, Nuclear Instruments and Methods in Physics Research A, 692, 201

Franceschini, A., Rodighiero, G., & Vaccari, M. 2008, A&A, 487, 837

Fritz, K. D. 1989, A&A, 214, 14

Gehrels, N. 1986, ApJ, 303, 336

Grondin, M.-H., Romani, R. W., Lemoine-Goumard, M., et al. 2013, ApJ, 774, 110

Hastings, W. K. 1970, Biometrika, 57, 97

Hewitt, J. W., Grondin, M.-H., Lemoine-Goumard, M., et al. 2012, ApJ, 759, 89

Lefa, E., Kelner, S. R., & Aharonian, F. A. 2012, ApJ, 753, 176

Mattox, J. R., Bertsch, D. L., Chiang, J., et al. 1996, ApJ, 461, 396

Nolan, P. L., Abdo, A. A., Ackermann, M., et al. 2012, ApJS, 199, 31

Stawarz, Ł., & Petrosian, V. 2008, ApJ, 681, 1725

Supanitsky, A. D., & Rovero, A. C. 2012, Astroparticle Physics, 36, 123

Szanecki, M., Bernlöhr, K., Sobczyńska, D., et al. 2013, Astroparticle Physics, 45, 1

Tam, P. H. T., Huang, R. H. H., Takata, J., et al. 2011, ApJ, 736, L10

Wehrle, A. E., Marscher, A. P., Jorstad, S. G., et al. 2012, ApJ, 758, 72

Zirakashvili, V. N., & Aharonian, F. 2007, A&A, 465, 695